Equivalent offset migration in anisotropic media

Pavan Elapavuluri and John C. Bancroft

ABSTRACT

Equivalent offset time migration has been shown to be a very effective migration technique. In its simplest form, this method assumes that the source/receiver traveltimes, or prestack diffraction shape of a scatterpoint, is defined by the double square-root (DSR) equation. The DSR equation usually assumes a hyperbolic definition of the source and receiver ray times based on the root-mean-squared (RMS) velocities. The equivalent offset is then defined by equating the DSR equation to a hyperbolic equation in which the offset is defined to be the equivalent offset. This method is fast and yields accurate velocities.

Applications of the equivalent offset (EO) method to anisotropic media have involved depth migration techniques to define the source/receiver traveltimes that are equated to a hyperbolic equation that (again) contains the equivalent offset. Using the equivalent offset to sort data in a migration gather aids in the velocity analysis process. This method does not have a speed advantage as it requires traveltime computations of a typical depth migration.

Our objective is to combine anisotropic traveltime estimates into the DSR equation with EO time migration for more accurate imaging at fast computational speed.

This technique was first tested on a simple anisotropic numerical model and then on a data set acquired over physical anisotropic model. An advantage of this method is that we can migrate data without the explicit information of anisotropy parameters.

INTRODUCTION

The velocity structure of the earth is fundamentally anisotropic, i.e. the velocity varies with the direction of propagating of energy. Imaging algorithms which are used to image seismic data need to take into account the velocity anisotropy.

It has been shown by various workers that the presence of anisotropy introduces errors into the final migrated image (Tsvankin, 2001; Nicola-Carena, 1997; Leslie et al., 1997; Vestrum and Lawton, 1999) etc. Larner and Tsvankin (1995) was one of the first papers to explore the imaging problems in anisotropic media. The most common imaging distortion induced by anisotropy is the inaccurate depth and lateral positioning, and in the case of prestack imaging, poor focusing of dipping and horizontal reflections (Vestrum et al., 1999b).

Isaac and Lawton (1999a) constructed a scaled physical model to investigate the magnitude of imaging errors incurred by the use of isotropic processing methods. They showed that isotropic prestack depth migration velocity analysis based upon obtaining consistent depth images in the common-offset domain results in the base of the anisotropic section being imaged 50 m (about 3%) too deep.

It has been commonly observed that in various geological settings there is the presence of dipping clastic sequences, which in many cases lie above the reservoir or targets, and most of these dipping clastic sequences have been observed to be anisotropic. (Isaac and Lawton, 1999b). According to Vestrum et al. (1999b) a dipping anisotropic strata overlying a target of interest can be characterized as a lens for propagating seismic energy. Below this lens, dipping as well as horizontal reflectors at boundaries between isotropic strata will be incorrectly positioned if isotropic models are assumed during data processing, particularly depth migration.

Isotropic depth migration corrects imaging problems and positioning errors associated with lateral, isotropic and velocity heterogeneities, but anisotropic depth migration is required to correctly locate images when transversely isotropic (TI) strata with a dipping axis of symmetry are present. In TI media P-wave seismic velocity is constant in all directions parallel to the bedding and typically slower in all the other directions. When dipping anisotropic strata are present in the overburden, the axis of symmetry are no longer horizontal and vertical. If the imaging algorithm doesn't account for this phenomenon, the resultant image may contain mis-positioning errors below.

Workers like Larner and Cohen (1993) and Alkhalifah et al. (2000) document migration errors in TI media. Uzcategui (1995) and Alkhalifah and Larner (1994) address the problem of depth imaging in the presence of VTI. Kitchenside (1991), Ball (2000), and Vestrum et al. (1999a) address seismic imaging in the presence of tilted transversely isotropic (TTI) media. Isaac and Lawton (2002) show dramatic positioning errors of horizontal reflectors below TI media with a tilted symmetry axis. Uren et al. (1990) discussed the lateral shift on zero-offset physical modeling data and the offset-dependent lateral shift on multichannel numerical data for a model similar to ours.

Various algorithms have been suggested for migrating in VTI media. The major ones are phase shift and Gaussian-Beam migrations by Alkhalifah (1995). Meadows and Abriel, (1994), have worked in developing VTI migrations based on Gazdag migration technique (Gazdag and Sguazzero, 1984).

Kirchhoff based depth migrations for VTI media were developed by the Ball (1995). Kirchhoff depth migrations need the traveltimes to be calculated for the model, these traveltimes can be calculated by solving the Eikonal equation, among many other techniques.

In this study we will be using Equivalent Offset Migration (EOM) to time migrate data with anisotropy present.

MIGRATION

The purpose of migration is to construct an image of the subsurface by transforming the information in the seismograms from the data space to an 'image space' (Geiger and Bancroft, 1996).

The final migrated images can be displayed either in 'time' or 'depth'. Depth migrations need an accurate velocity model, which is difficult to build, therefore time migrations are more common and widely used.

TIME MIGRATION

In the above section we defined the migration as the transformation from data space to image space. Time migration can be defined as the technique which transfers the data space to image space with a vertical dimension of time. Yilmaz (2000) supports this by stating "the migration process that produces a migrated time section is called a time migration". Time migration assumes the diffraction shape to be hyperbolic and collapses the energy to the apex of hyperbola.

There are many advantages of time migration; they are (Bancroft, 1997):

- The method is very robust, i.e. the errors in the velocity model have very little effect on the migrated image as they effect focusing of the data not the position,

- Time migration is also widely used to refine the velocity model; when the velocity model is considered accurate enough, this velocity model can be used to for depth migration,

- The unmigrated section and prestack time migrated section appear quite similar to the position of the data, making it easier to compare the quality of migrations,

- The accuracy of velocities can be around 3 to 10%,

- Complex structures in the shallower part of the section, don't effect the migration of the data below, and

- It's computationally faster.

The disadvantages of time migrations are (Bancroft, 1997):

- The output is in time, not depth,

- Structured data may not be positioned correctly,

- Time migration may not position dipping data, as accurately as depth migration, and

- Might not focus structurally complex data.

Time migration can be applied both before and after stacking the seismic data. In this paper we will be dealing exclusively with prestack time migration. There are various methods of time migration, the following are widely used:

- Kirchhoff time migration,

- Phase shift methods, and

- Equivalent Offset Method.

We will be extending the equivalent offset technique proposed by Bancroft (1997) to include anisotropic media.

KIRCHHOFFMIGRATION

Kirchhoff migration can be applied by assuming a scatter point location, defining the diffraction shape and position, then summing the energy along the diffraction path, and relocating the energy at the scatter point.

The traveltime t of a diffraction shape from a scatter point in (x, h, t) space is defined by the equation (1), commonly known as the double-square-root (DSR) equation:

$$t = \sqrt{\frac{t_0^2}{4} + \frac{(x+h)^2}{v_{rms}^2}} + \sqrt{\frac{t_0^2}{4} + \frac{(x+h)^2}{v_{rms}^2}} \ , \tag{1}$$

where t_0 is the two-way time from the scatter point, x is the horizontal distance from the scatter point to the CMP, h is the half offset, and v_{rms} is the root-mean-squared (rms) velocity. Pictorially equation (1) represents a surface is known as Cheops Pyramid (Ottolini and Claerbout, 1984). Hyperbolic intersections are formed when number of planar surfaces intersect Cheops pyramid. The Kirchhoff time migration of source records involves summing along this hyperbolic diffraction surface. Kirchhoff time migration is usually used when the velocities are varying smoothly and also as a starting point to build a detailed structural velocity model for depth migration. Time migration is also used to image the media where the structure is too complex for depth migration (Bancroft, 1997). It is to be noted that equation (1) shows that the diffraction in time domain is defined by the rms velocity.

Time migration does not position the migrated data correctly when there are lateral velocity variations. The velocity model as described earlier should be sufficiently smooth for Kirchhoff time migration to work properly.

EQUIVALENT OFFSET MIGRATION

Equivalent offset migration (EOM) is a modified form of Kirchhoff migration and it can be both a time and depth migration. The EOM method moves the input sample directly to the equivalent offset (EO) gather.

The method computes the location of a colocated source and receiver that maintains the same travel time t to a scatter point as the original source and receiver as shown in the Figure 1.

The offset from the scatter point to the collocated source and receiver is defined as h_e. It is found by equating the DSR equation to a hyperbolic equation that contained h_e as the offset parameter, i.e.,

$$t(x) = \sqrt{\frac{t_0^2}{4} + \frac{(x+h)^2}{v_{rms}^2}} + \sqrt{\frac{t_0^2}{4} + \frac{(x+h)^2}{v_{rms}^2}} = 2\sqrt{\frac{t_0^2}{4} + \frac{h_e^2}{v_{rms}^2}} \tag{2}$$

where t_0 is the zero offset vertical travel time, v_{rms} is the rms velocity, x is the distance between the scatter point and the CMP, and h is half offset. These parameters are illustrated in the Figure 1. The EO term h_e can be derived and written as:

$$h_e = x^2 + h^2 - \frac{4x^2h^2}{t^2v^2}.$$

(3)

This formulation reduces the complex shape of the DSR equation into a simple hyperbola.
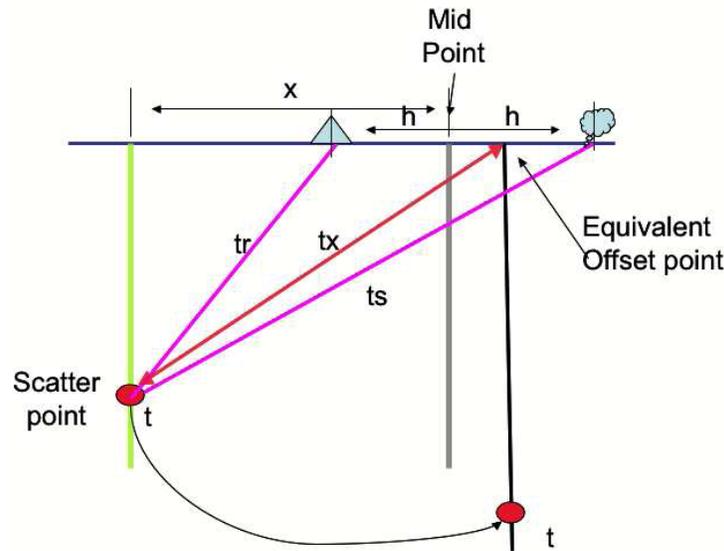
FIG. 1. The ray paths to scatter point.

EQUIVALENT OFFSET MIGRATION IN ANISOTROPIC MEDIA

Equation (1) gives the diffraction surface due to a scatter point in an isotropic media. In the case of generalized anisotropic media it has been shown by Tsvankin (2001) that the moveout is no longer hyperbolic but essentially non-hyperbolic. This non-hyperbolic nature increases as the offset increases. Therefore the hyperbolic treatment of prestack migration is limited to smaller offsets.

We restrict the term "hyperbolic moveout" to the case of linear rays on a time section that travel between the surface ($x = 0$ and $t = 0$) and a scatterpoint. The traveltimes of these rays are computed as individual raypaths and summed to form equation (1), as illustrated in Figure 1. In this context, a hyperbola that is bulk shifted in time relative to t and t_0 will be considered to have non-hyperbolic moveout.

DSR equation for anisotropic media

The DSR equation (2) is valid in isotropic homogeneous media and has been shown by Bancroft (1997) to be valid in heterogeneous media for shorter offsets.

In anisotropic media, even for shorter offsets, the diffraction shape is no longer hyperbolic (Tsvankin, 2001). In order to extend this method of Kirchhoff summation

technique to anisotropic media, the diffraction summation hyperbola is made non-hyperbolic. We propose that the diffraction shape be made non-hyperbolic by using the shifted hyperbola technique proposed by Castle (1994). The two-way travel time t_{sh} of energy from a scatter point in anisotropic media can be written with a shifted hyperbola:

$$(t_{sh} - \tau_s)^2 = (t_0 - \tau_s)^2 + \frac{4h^2}{V_{rms}^2},$$ (4)

where τ_s is the time shift of the hyperbola and h is either the source offset $h_s = x + h$ or receiver offset $h_r = x - h$ as implied in Figure 1. Castle introduces a shift parameter s defined as:

$$s = \frac{t_0}{t_0 - \tau_s},$$ (5)

to formulate the shifted hyperbola equation as:

$$t_{sh} = t_0 \left(1 - \frac{1}{s}\right) + \sqrt{\left(\frac{t_0}{s}\right)^2 + \frac{4h^2}{sV_{rms}^2}}.$$ (6)

The DSR equation may now be written using one-way times for the source and receiver raypaths as:

$$t = t_{sh-s} + t_{sh-r} = \frac{t_0}{2}\left(1 - \frac{1}{s}\right) + \sqrt{\left(\frac{t_0}{2s}\right)^2 + \frac{h_s^2}{sV_{rms}^2}} + \frac{t_0}{2}\left(1 - \frac{1}{s}\right) + \sqrt{\left(\frac{t_0}{2s}\right)^2 + \frac{h_r^2}{sV_{rms}^2}}$$ (7)

Equivalent offset in anisotropic media

The focusing of EOM may be improved if the non-hyperbolic moveout is used in the DSR equation, which is then is equated to a equivalent offset hyperbolic equation in,

$$t_0\left(1 - \frac{1}{s}\right) + \sqrt{\left(\frac{t_0}{2s}\right)^2 + \frac{h_s^2}{sV_{rms}^2}} + \sqrt{\left(\frac{t_0}{2s}\right)^2 + \frac{h_r^2}{sV_{rms}^2}} = t = 2\sqrt{\left(\frac{t_0}{2}\right)^2 + \frac{h_e^2}{V_{rms}^2}}.$$ (8)

We don't solve for h_e in terms of the DSR parameters, but instead we use the two-way traveltime t, i.e.,

$$h_e = \frac{v_{rms}}{2}\sqrt{(t^2 - t_0^2)}.$$ (9)

Algorithm

The application of EOM using the shifted hyperbola approach is very similar to the conventional approach. The only additional step is to calculate the "shift" parameter.

Equivalent offset gathers in anisotropic media can be formed using the following technique:

- Estimate velocity and shift parameter,

- calculate shifted hyperbola travel time,

- calculate equivalent offset,

- sort the data into equivalent offset gathers using equation (9), and

- apply scaling and NMO to these gathers.

The advantage of using this technique is that the non-hyperbolic diffractions will be forced into a hyperbolic shape with the rms velocities. A conventional moveout correction algorithm can be used to correct for the moveout and then the gathers are weighted and stacked to accomplish prestack time imaging.

EXTENDED ANISOTROPIC EQUIVALENT OFFSET METHOD

The shifted hyperbola approach works well for moderately non-hyperbolic diffractions and for data with shorter offsets. We further modify the method to include longer offsets with increase non-hyperbolic characteristics. This is achieved by making the "shift" parameter dependent of the offset.

Castle (1994) has shown that for larger offsets and higher moveout, the shift parameter can be written as a function of offset. This function can be written as:

$$s(h) = \frac{\tilde{a} + sh^2}{\tilde{b} + sh^2} . \qquad (10)$$

We found that this equation is cumbersome to calculate, so it is approximated as a polynomial of offset:

$$s(h) = s + ah + bh^2 , \qquad (11)$$

where *a* and *b* are constants. The parameters *s*, *a* and *b* can be determined by performing a simulated annealing inversion on the traveltimes verses offset data (Elapavuluri and Bancroft, 2002). The extended EOM technique is applied using the same procedure as in the earlier shifted hyperbola based EOM approach. The technique can applied using the following steps:

- Estimate velocity *s*, *a* and *b*,

- calculate shifted hyperbola travel time,

- calculate equivalent offset,

- sort the data into equivalent offset gathers, and

- apply scaling and NMO to these gathers.

TESTING ON A SIMPLE MODEL

The above discussed technique is applied to a very simple model with a single anisotropic layer as shown in Figure 2. The model parameters of the anisotropy layer are $v_0 = 3000$ m/s, $\varepsilon = 0.2$ and $\delta = -0.2$. CMP gathers were formed on the model. Figure 3 shows a two-sided CMP gather formed at the center of the model. Semblance analysis is performed on this CMP gather and displayed in Figure 4. The CMP gathers are then normal moveout (NMO) corrected and displayed in Figure 5.
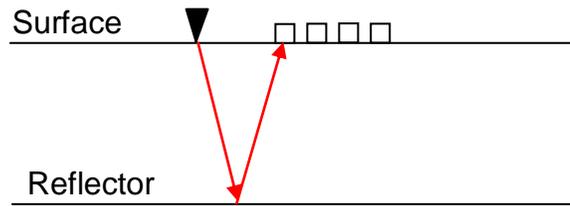
FIG. 2. The 2D model.
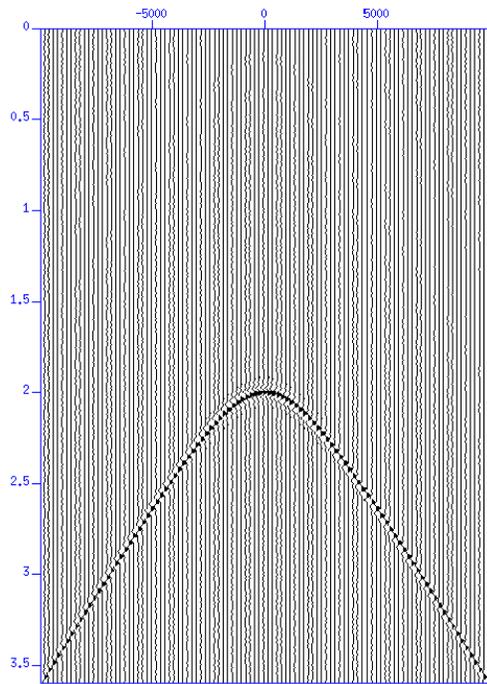
FIG. 3. A CMP gather in the middle of the model.
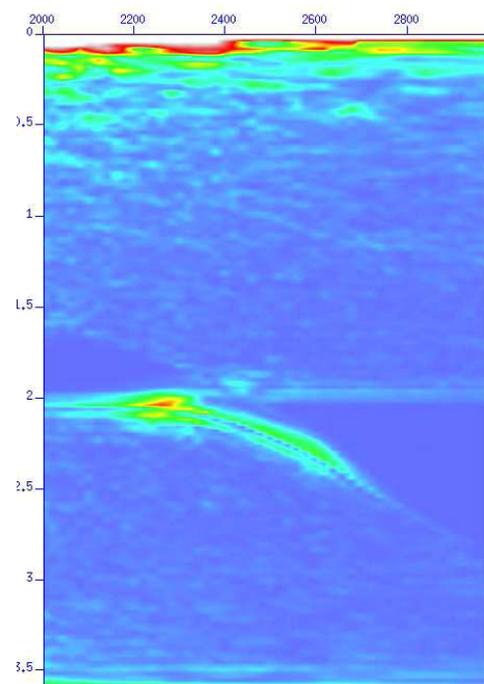
FIG. 4. Semblance over the CDP gathers.
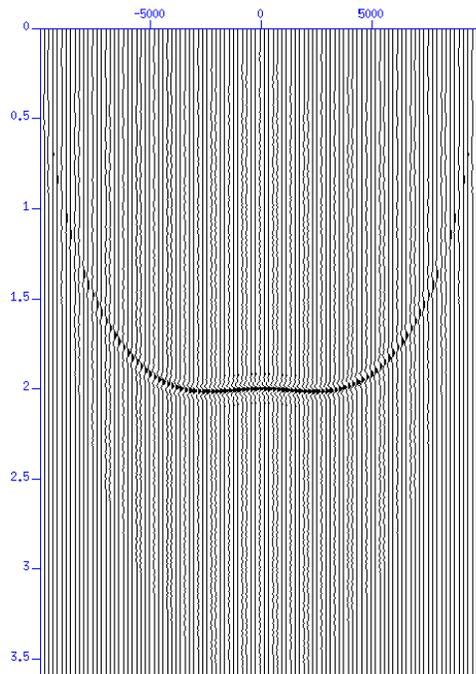
FIG. 5 NMO corrected CDP gather.

It can be observed that from the NMO corrected gather that instead of the time being constant for all offsets, the time decreases with offset, exhibiting a typical 'hockey stick phenomenon' when this data is stacked, the data will be both temporally and spatially miss-positioned.

Equivalent offset gather (isotropic)

An equivalent offset gather is formed at the middle of the model is shown in the Figure 6. Semblance is calculated on this EO gather and is displayed in Figure 7. Using the velocity estimated from the semblance plot the EO gather is NMO corrected and shown in Figure 8.

It can be observed in the semblance plot that the energy is not focused and there remains trailing energy. Selecting an optimal stacking velocity will be a problem. In isotropic EO moveout corrected gather we find that the anisotropic event still shows the hockey stick moveout effect.
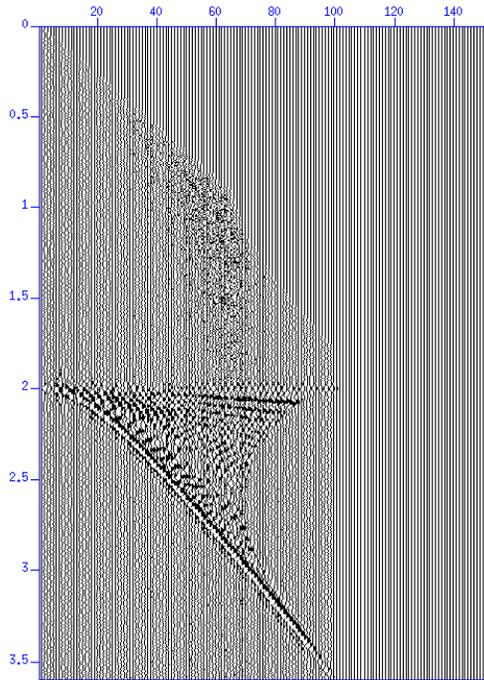
FIG. 6. A normal EO Gather.
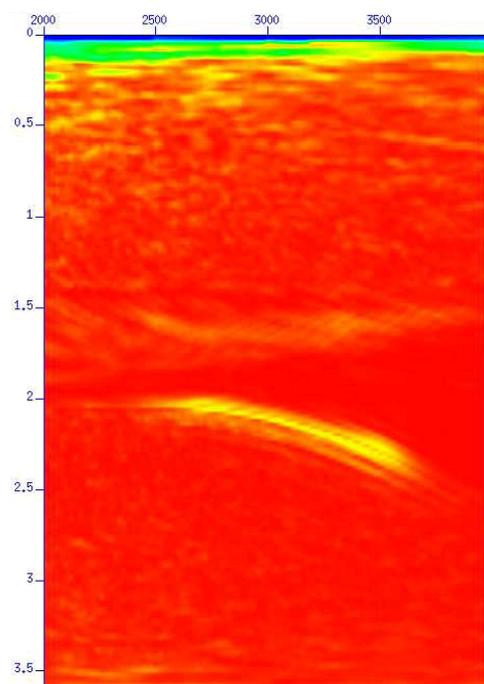
FIG. 7. Semblance analysis of normal EO gathers.
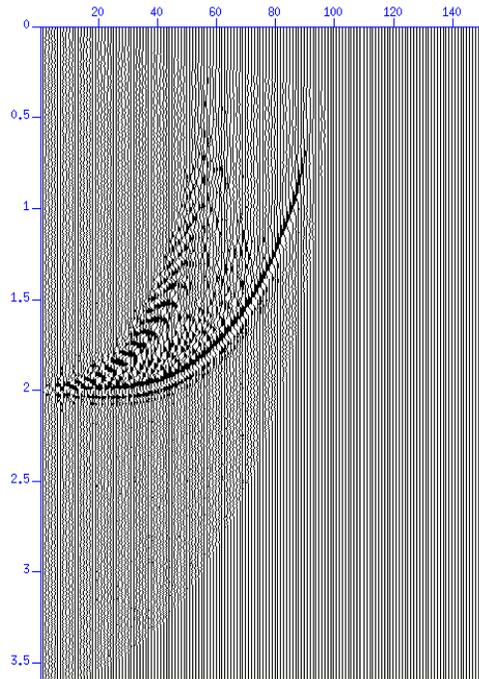
FIG. 8. NMO corrected normal EO gather.

Anisotropy EO gathers

Anisotropic EO gather technique is applied on this data. Before applying this data we have to estimate the values of *s*, *a,* and *b* as shown in Elapavuluri and Bancroft (2002). Using these estimated parameters the anisotropic EO gather is formed and is shown in Figure 9. Semblance analysis is performed on this gather and showed in Figure 10. It can be seen in the semblance analysis that the energy is more focused and is easies to pick the NMO velocity in contrast to using just the CMP gather or the conventional EO gather.

Using the velocity estimated from the semblance analysis the EO gather is NMO corrected and shown in the Figure 11. It can be observed that the NMO corrected gather is straighter and there is little residual moveout.

The same process is applied to all the EO gathers formed through out the model, these are then NMO corrected and stacked, thus producing the prestack migrated image as shown in the Figure 12.
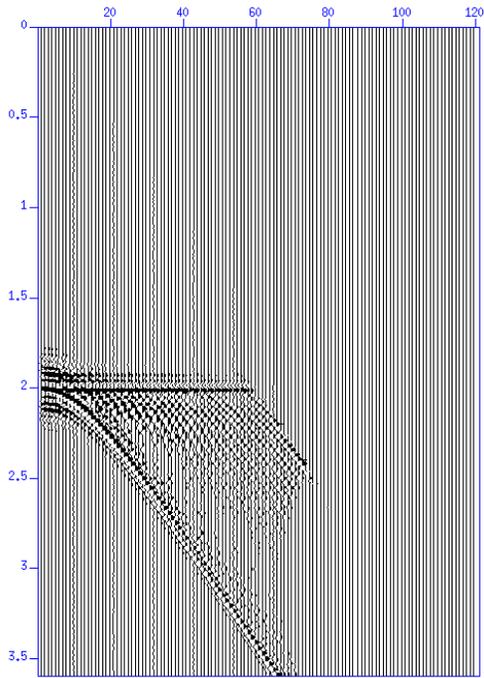
FIG. 9. Anisotropic EO gather formed with variable shift.
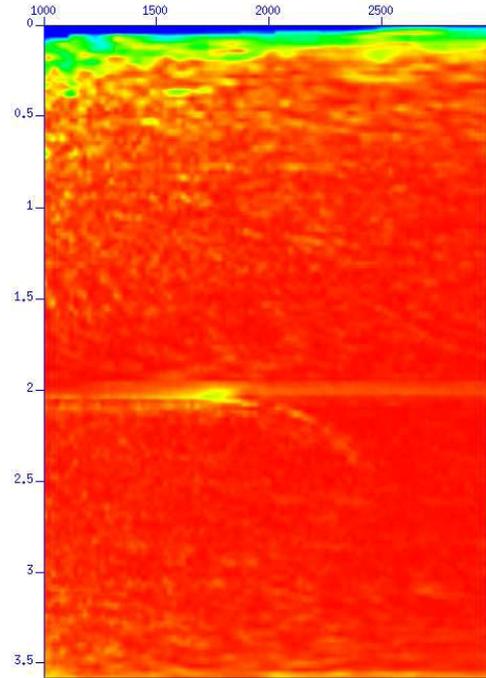
FIG. 10. Semblance over the anisotropic EO gather.
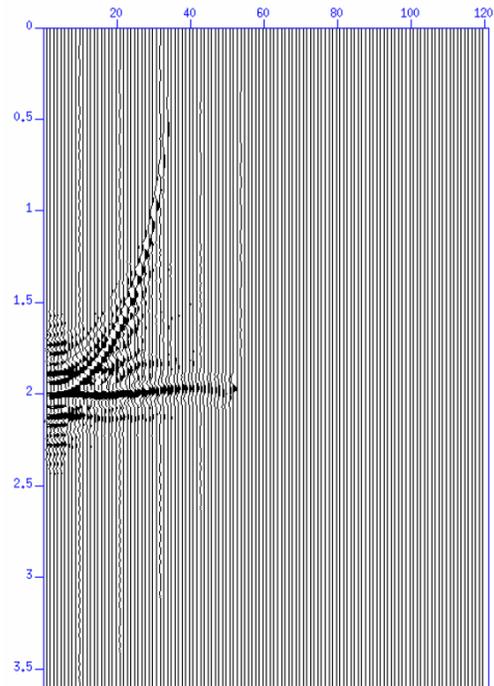
FIG. 11. NMO corrected anisotropic EO gather.
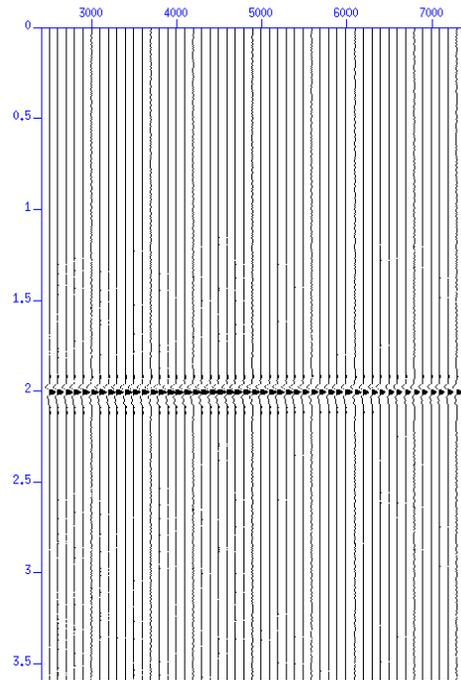
FIG. 12. Migrated section.

PHYSICAL MODELLING DATA

Leslie and Lawton (2001) acquired seismic data over a physical model of an anisotropic thrust sheet. The physical model is illustrated in Figure 13. This model consists of a flat reflector overlain by a TI thrust sheet embedded in an isotropic background. The thrust sheet is composed of four blocks in the model; each with a unique axis of symmetry. They have parameters of $v_{p0} = 2925$ m/s, $\varepsilon = 0.2$, and $\delta = 0.1$. The isotropic background has $v_{p0} = 2740$ m/s.

The algorithm described above is now tested on this model. The objective of this study is to see how anisotropy influences the imaging in anisotropic media and the pitfalls one should be careful when dealing with such data.
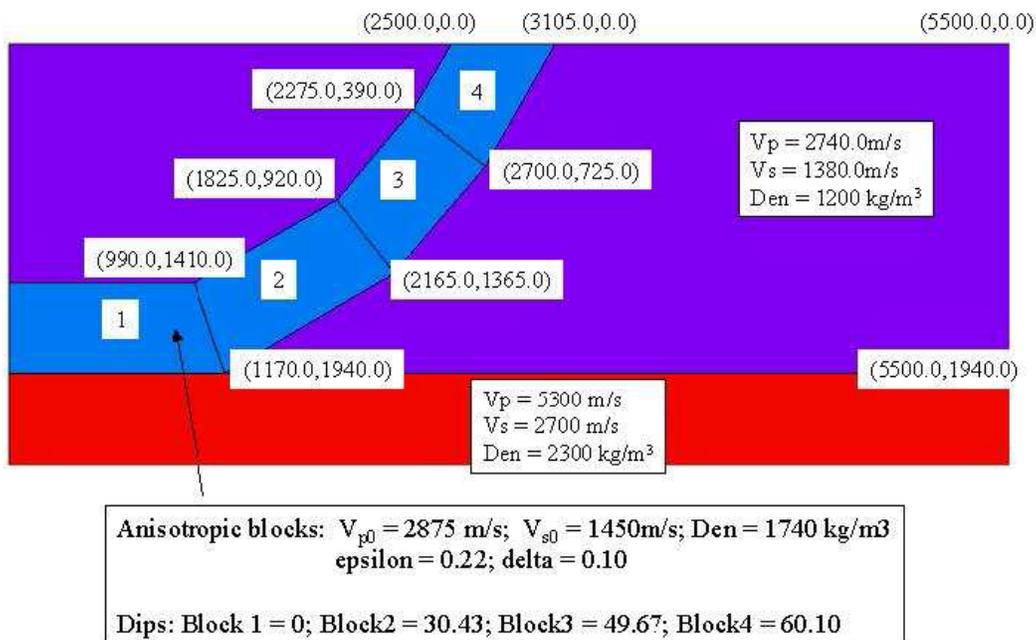
FIG. 13. Thrust sheet model (Courtesy Don Lawton).

Figure 14 shows a shot at the middle of the survey. The data is then sorted into CMP gathers. Figure 15 shows a CMP gather at the middle of the survey. Semblance analysis is performed on this gather and is shown in the Figure 16.
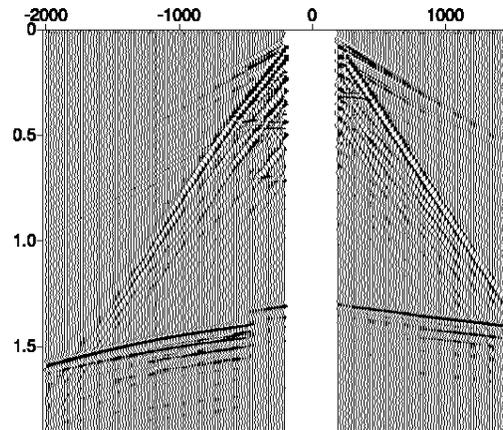
FIG. 14. A shot from the middle of the data.

KIRCHHOFF TIME MIGRATION

This data is first migrated using conventional Kirchhoff time migration technique using a velocity model built from conventional semblance analysis.

The final migrated image is shown in Figure 17. It can be seen that the thrust sheet upper limbs of the thrust sheet are imaged fairly well.

The basement at 1.4 s, which is supposed to be flat is in fact flat everywhere else, except directly under the thrust sheet.
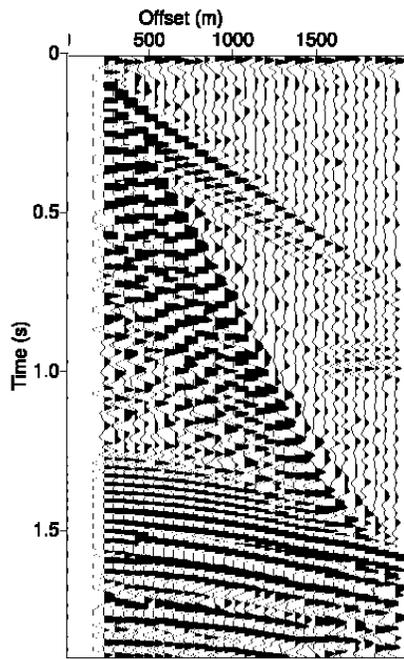
FIG. 15. CMP at middle of the data.
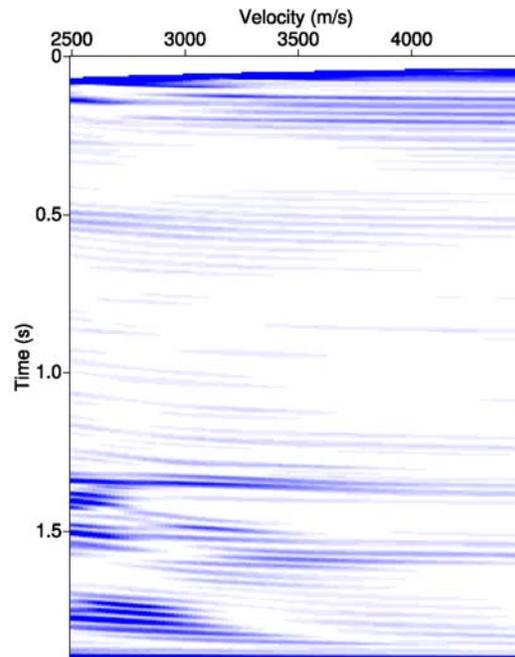
FIG. 16. Semblance at the middle of the data.
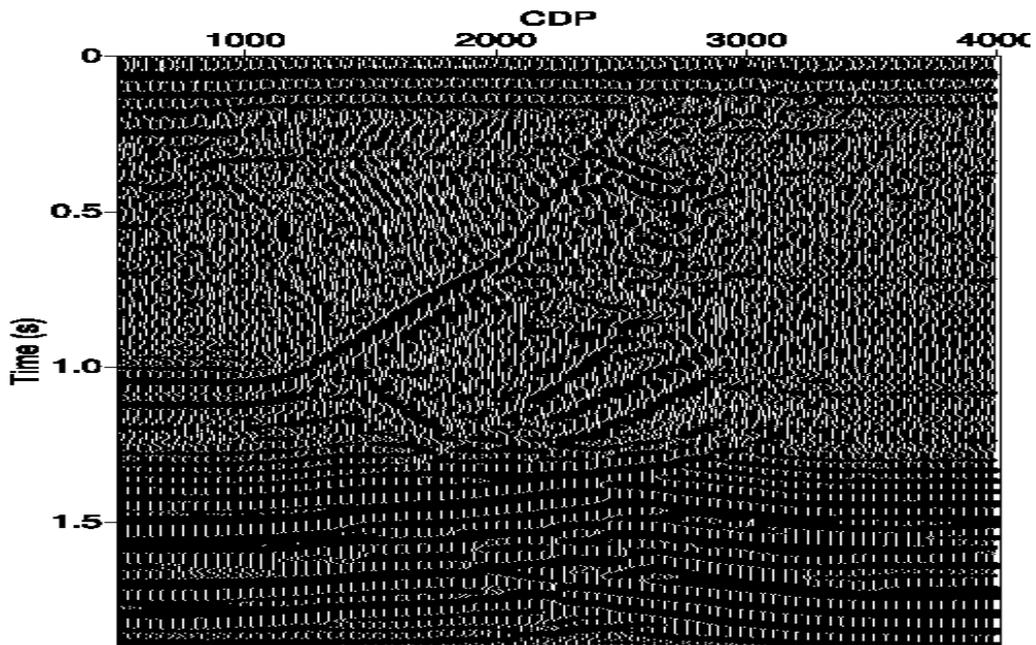
FIG. 17. Kirchhoff time migrated image.

EQUIVALENT OFFSET MIGRATION

The same data is migrated using normal EOM. The technique is discussed above. EO gathers are formed on this data and then semblance analysis is performed on this data. The data is sorted into normal EO gathers, Figure 18 shows the CMP gather at the middle of the survey. Semblance analysis is performed on this gather and is shown in the Figure 19.

The data is NMO corrected and stacked. The final migrated image is shown in Figure 20.

It is apparent that the results of Prestack Kirchhoff imaging Figure 17 and EOM Figure 20 are very comparable to each other, both have the three limbs imaged well and they have the upwelling of the basement under the thrust sheet.
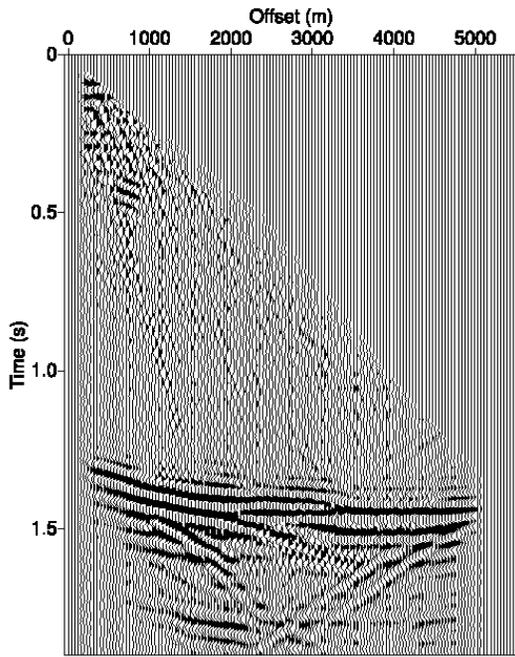
FIG. 18. A normal EO gather from the middle of the data.
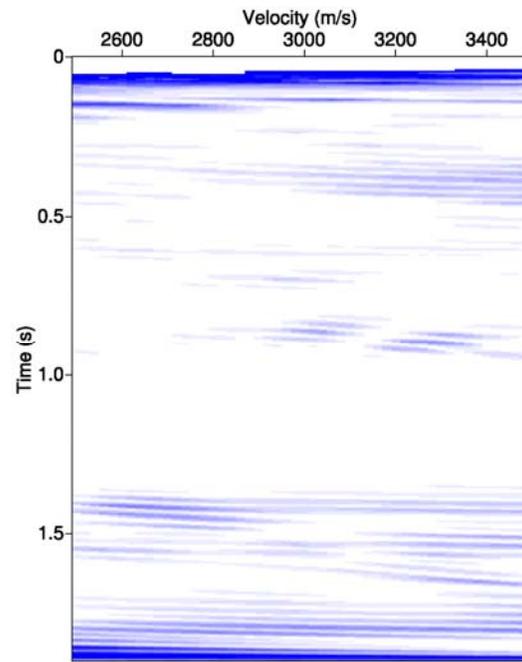
FIG. 19. Semblance plot of the normal EO gather.
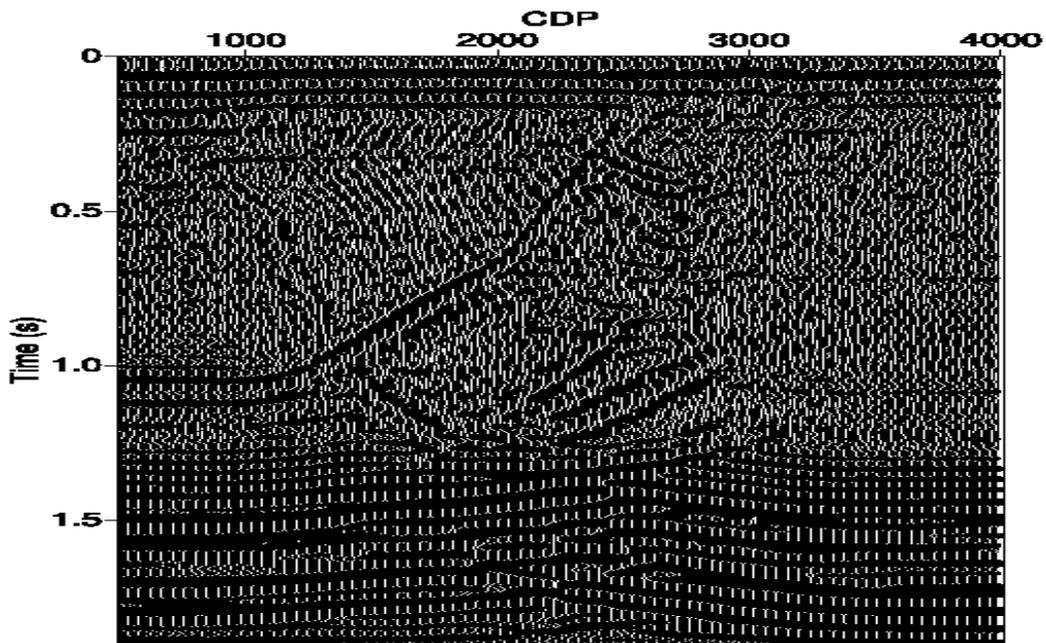
FIG. 20. Prestack migrated image using normal EOM.

ANISOTROPIC EQUIVALENT OFFSET MIGRATION

Anisotropic EOM is now applied to this data; the first step is to estimate the shift parameters *s*, *a*, and *b*. The estimation technique is discussed in detail in (Elapavuluri and Bancroft, 2004). Using these estimated parameters anisotropic EO gathers are formed using the data collected over the data.

The EO gathers are then NMO corrected and stacked to form a Prestack migrated section shown in Figure 21. The most interesting section is under the thrust sheet where there is upwelling is evident in other migrations. Now zooming into this interesting section we can see that there is no artifact due to anisotropy.

The section as in the other two cases the limbs are imaged well but the improvement is in the imaging of the basement; it is flatter through out and there is little upwelling in the basement. It has to be emphasized that no where in the imaging processes we have used explicit information about the anisotropy parameters in the model.
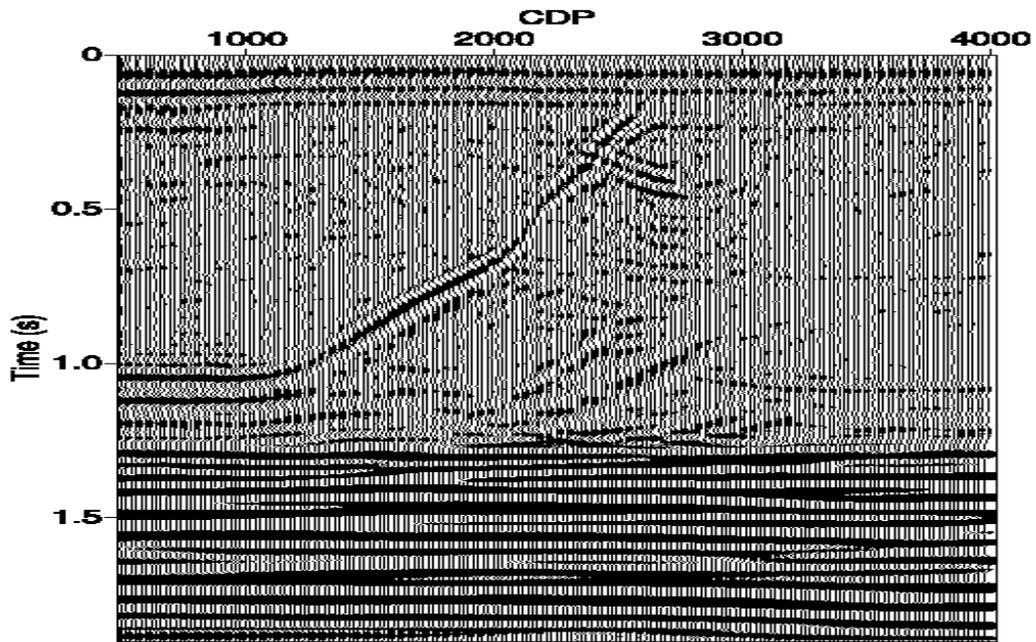
FIG. 21. Prestack migrated image using anisotropic EOM.
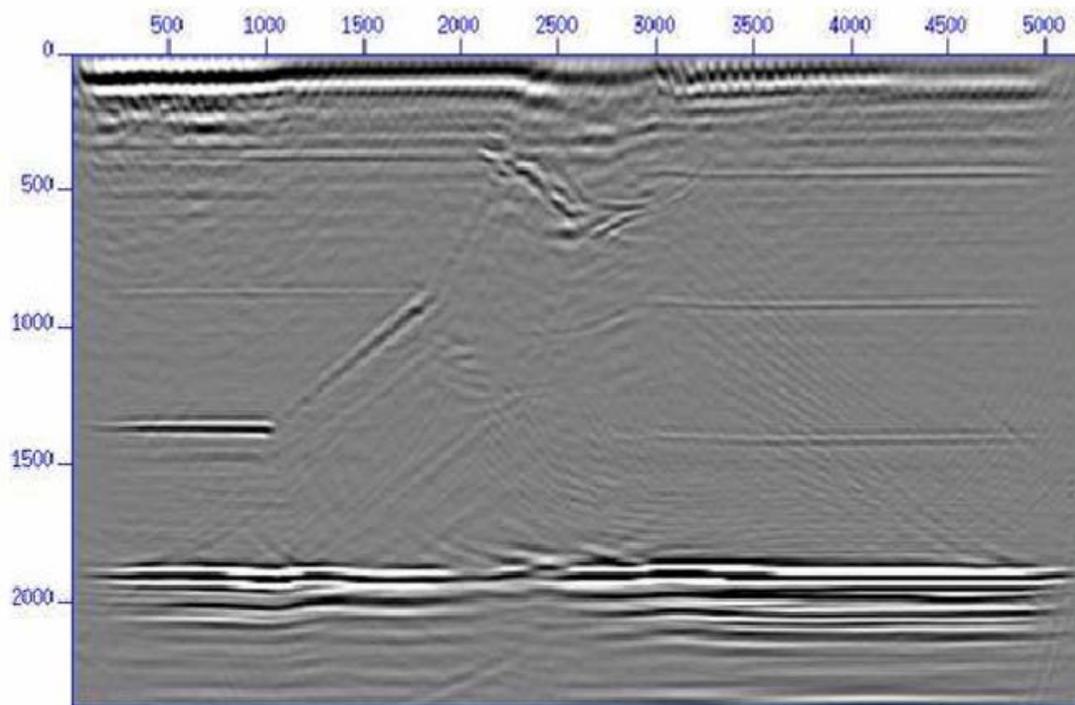
FIG. 22. Prestack migrated image using PSPI migration, courtesy Xiang Du.
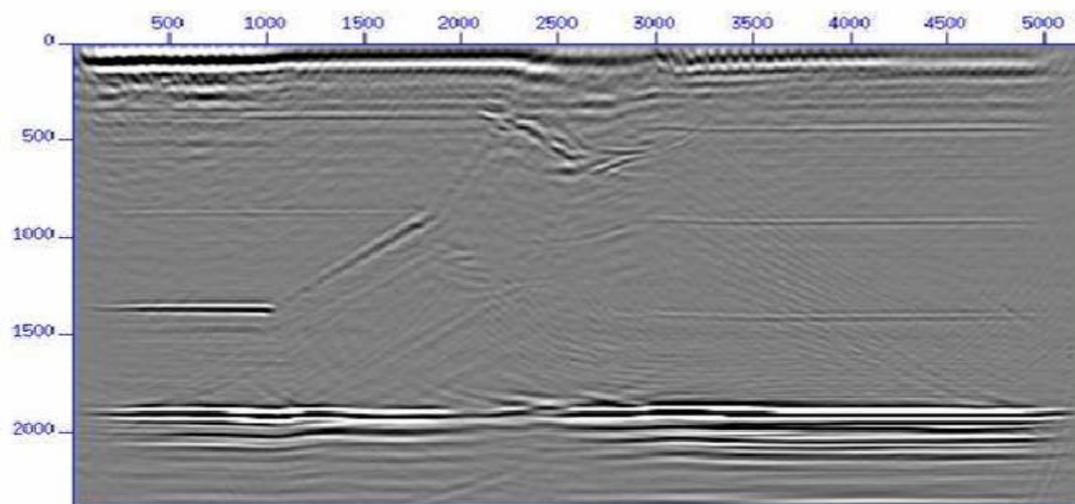
FIG. 23. Prestack migrated image using reverse time migration courtesy Xiang Du.

COMPARISON

Many workers have worked on imaging this data in depth using various techniques. Notable are (Ferguson and Margrave, 1998), (Kumar and Ferguson, 2004) and (Du, 2006). Du (2006) image this data using reverse time migration. He compares his results to the results obtained using PSPI technique (Gazdag, 1978).

Figure 22 shows the depth migrated image for the thrust sheet model using PSPI technique and Figure 23 shows the depth migrated imaging produced using reverse time

migration. The reverse time migrated image Figure 23 images all the limbs without the artifact beneath the anisotropic thrust sheet.

Comparing the migrated sections Figures 21 and 23 produced by anisotropic EOM and reverse time migration can be seen that both are comparable to each other. All the limbs are imaged properly and mainly the basement remains flat without any upwelling.

CONCLUSIONS

In this paper we have shown that non-hyperbolic diffraction can be approximated by a Shifted hyperbola equation. We have extend Equivalent offset migration to anisotropic media. We have also proposed a technique by which data with anisotropy present in it can be migrated in time domain without the knowledge of anisotropy parameters.

We tested this technique on a simple 2D model and then applied this technique to thrust sheet data with TTI present in the thrust sheet. The time migrated image is shown to image the basement better than the traditional Kirchhoff time migration and normal EOM. This data is then showed that it's comparable in quality to a reverse time depth migrated image.

REFERENCES

Alkhalifah, T., 1995, Gaussian beam depth migration for anisotropic media: Geophysics, **60**, No. 05, 1474–1484.

Alkhalifah, T., Batzle, M., Larner, K., Christiansen, R., and Han, D., 2000, Migration error in transversely isotropic media, *in* Applied seismic anisotropy: theory, background, and field studies, Soc. of Expl. Geophys., **20**, 204–217.

Alkhalifah, T., and Larner, K., 1994, Migration error in transversely isotropic media: Geophysics, **59**, No. 09, 1405–1418.

Ball, G., 1995, Estimation of anisotropy and anisotropic 3-D prestack depth migration, offshore Zaire: Geophysics, **60**, No. 05, 1495–1513.

Ball, G., 2000, Estimation of anisotropy and anisotropic 3-D prestack depth migration, offshore Zaire, *in* Applied seismic anisotropy: theory, background, and field studies, Soc. of Expl. Geophys., **20**, 637–655.

Bancroft, J. C., 1997, A practical understanding of pre- and poststack migrations, Soc. of Expl. Geophys., 409.

Castle, R. J., 1994, Theory of normal moveout: Geophysics, **59**, No. 06, 983–999.

Du, L. L., Bancroft, 2006, Two Prestack Anisotropic Depth Migration Methods for Tilted TI Media, 82–82.

Elapavuluri, P., and Bancroft, J., 2002, Estimation of Thomsen's Anisotropic Parameters Using Shifted Hyperbola NMO Equation, *in* 64th Mtg., Eur. Assn. Geosci. Eng., P134.

Elapavuluri, P., and Bancroft, J., 2004, Inversion for Thomsen's anisotropy parameters: Preview, **111**, 77.

Ferguson, R. J., and Margrave, G. F., 1998, Depth migration in TI media by non-stationary phase shift, *in* 68th Ann. Internat. Mtg, Soc. of Expl. Geophys., 1831–1834.

Gazdag, J., 1978,Wave equation migration with the phase-shift method: Geophysics, **43**, No. 07, 1342–1351.

Gazdag, J., and Sguazzero, P., 1984, Migration of seismic data by phase-shift plus interpolation: Geophysics, **49**, No. 02, 124–131.

Geiger, H. D., and Bancroft, J. C., 1996, Equivalent offset prestack migration for rugged topography, *in* 66th Ann. Internat. Mtg, Soc. of Expl. Geophys., 447–450.

Isaac, J. H., and Lawton, D. C., 1999a, Image mispositioning due to dipping TI media: A physical seismic modeling study: Geophysics, **64**, No. 4, 1230–1238.

Isaac, J. H., and Lawton, D. C., 1999b, Image mispositioning due to dipping TI media: a physical seismic modeling study, *in* Depth imaging of foothills seismic data, Soc. of Expl. Geophys., 215–223.

Isaac, J. H., and Lawton, D. C., 2002, Image mispositioning in foothills seismic data due to a dipping transversely isotropic overburden: Implications from physical seismic modelling studies: Recorder, **27**, No. 3, 34–38.

Kitchenside, P.W., 1991, Phase-shift based migration for transverse isotropy, *in* 61st Ann. Internat. Mtg, Soc. of Expl. Geophys., 993–996.

Kumar, M. K. S., D., and Ferguson, R. J., 2004, Traveltime calculation and prestack depth migration in tilted transversely isotropic media, *in* Geophysics, vol. 69, Soc. of Expl. Geophys., 37–44.

Larner, K., and Cohen, J. K., 1993, Migration error in transversely isotropic media with linear velocity variation in depth: Geophysics, **58**, No. 10, 1454–1467.

Larner, K., and Tsvankin, I., 1995, P-wave anisotropy: Its practical estimation and importance in processing and interpretation of seismic data, *in* 65th Ann. Internat. Mtg, Soc. of Expl. Geophys., 1502–1505.

Leslie, J.M., and Lawton, D. C., 2001, P-wave traveltime anomalies below a dipping anisotropic thrust sheet, *in* Advances, Soc. of Expl. Geophys., 77–84.

Leslie, J. M., Lawton, D. C., and Cunningham, J. D., 1997, Anisotropic parameter determination of shales by a refraction seismic field study, *in* 59th Mtg., Eur. Assn. Geosci. Eng., Session: P093.

Meadows, M. A., and Abriel, W. L., 1994, 3-D poststack phase-shift migration in transversely isotropic media, *in* 64th Ann. Internat. Mtg, Soc. of Expl. Geophys., 1205–1208.

Nicola-Carena, E. D., 1997, Solving lateral shift due to anisotropy, *in* 67th Ann. Internat. Mtg, Soc. of Expl. Geophys., 1525–1528.

Ottolini, R., and Claerbout, J. F., 1984, The migration of common-midpoint slant stacks: Geophysics, **49**, No. 03, 237–249.

Tsvankin, I., 2001, Seismic Signatures and Analysis of Reflection Data in Anisotropic Media: Pergamon.

Uren, N. F., Gardner, G. H. F., and McDonald, J. A., 1990, The migrator's equation for anisotropic media: Geophysics, **55**, No. 11, 1429–1434.

Uzcategui, O., 1995, 2-D depth migration in transversely isotropic media using explicit operators: Geophysics, **60**, No. 06, 1819–1829.

Vestrum, R., and Lawton, D., 1999, Anisotropic depth migration: Reducing lateral-position uncertainty of subsurface structures in thrust-belt environments, *in* 69th Ann. Internat. Mtg, Soc. of Expl. Geophys., 1107–1109.

Vestrum, R.W., Lawton, D. C., and Schmid, R., 1999a, Imaging structures below dipping TI media, *in* Depth imaging of foothills seismic data, Soc. of Expl. Geophys., 224–231.

Vestrum, R. W., Lawyer, D. C., and Schmid, R., 1999b, Imaging structures below dipping TI media: Geophysics, **64**, No. 4, 1239–1246.

Yilmaz, O., 2000, Seismic Data Analysis, Soc. of Expl. Geophys., 1000.